Shock and Vibration 10 (2003) 59–69
IOS Press

A hybrid control policy for semi-active vehicle suspensions

Fernando D. Goncalves and Mehdi Ahmadian*
Advanced Vehicle Dynamics Laboratory, Department of Mechanical Engineering, Virginia Tech, Blacksburg, VA 24061, USA

Received 25 April 2002
Revised 23 May 2002

Abstract. Various control policies, such as skyhook and groundhook control, have often been considered for semi-active vehicle suspensions. Past studies have shown the performance limitations of these policies, as well as others that have been considered for vehicle applications. This study will provide a look into an alternative control technique called "hybrid control," which attempts to merge the performance benefits of skyhook and groundhook control. The results of this study are based on an experimental evaluation of hybrid control using a quarter-car rig and a magneto-rheological damper. The control policy is employed and evaluated under a steady-state or pure tone input, and a transient or step input. Peak-to-peak displacement and peak-to-peak acceleration are used to evaluate performance. The results indicate that hybrid control can offer benefits to both the sprung mass and the unsprung mass. The steady-state results reveal that hybrid control can be used to reduce the peak-to- peak displacements and accelerations of both bodies. The transient evaluation shows that hybrid control can be effective at reducing the peak-to-peak displacement of the sprung mass.

1. Introduction

As technology advances, semi-active suspensions continue to gain considerable attention. Semi-active suspensions consist of a spring element and a damper which offers variable damping. Whether through mechanically changing orifices or fluid with adjustable viscosity, a semi-active damper has the ability to adjust the damping level.

First introduced by Crosby and Karnopp [1,2], semi-active systems have since been considered for vehicle primary suspensions. Semi-active suspensions have been shown to offer valuable benefits for vehicle primary suspensions [3–7]. Moreover, semi-active suspension systems have developed into a technology that is currently being implemented. Available in the 2002 Cadillac Seville STS, the MagneRideTM semi-active suspension uses a magneto-rheological damper made by Delphi to vary the damping according to the driving conditions. Beyond improvements in ride and handling, Cadillac also claims that the system is very effective at slowing weight transfer, which promotes stability [8,9]. Maserati also offers a semi-active suspension that implements a newly developed Mannesmann Sachs skyhook control system in its 2002 Spyder. The system uses high-speed integrated proportional valves on each shock. Using six electronic sensors to control the body and individual wheel reactions to bumps, the semi-active suspension improves roadholding as well as handling and ride comfort. Maserati claims the system reduces the variation on wheel loadings by up to 50 percent [10,11]. This technology is current and clearly offers valuable applications for vehicle suspensions.

The benefits observed in the popular skyhook control are further extended to groundhook control. Where skyhook excels at controlling the suspended or sprung body, groundhook control excels at controlling the unsprung mass. An alternative semi-active control policy known as hybrid control has been shown to take advantage of the benefits of both skyhook and groundhook

*Corresponding author: Tel.: +1 540 231 4920; Fax: +1 540 231 9100; E-mail: ahmadian@vt.edu.

ISSN 1070-9622/03/$8.00

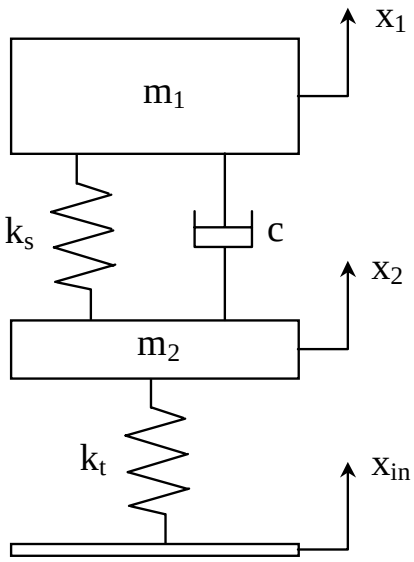

Fig. 1. 2DOF Quarter-Car Model.

control [12]. Comprehensive reviews of these semi-active control policies are available in the work by Ivers and Miller [13].

The focus of this work is to evaluate the benefits of hybrid control. Specifically, the transient and steady state performance of hybrid control will be evaluated. This experimental evaluation will be done using a test rig that emulates the single suspension model shown in Fig. 1. Since the model represents a single suspension from one of the four corners of a vehicle, this 2-degree of freedom (2DOF) system is often referred to as the "quarter-car" model. The mass of the vehicle body (sprung mass) and the tire/axle assembly (unsprung mass) are defined respectively by m_1 and m_2, with their corresponding displacements and velocities defined by x_1 and x_2, and v_1 and v_2, respectively. The relative velocity, v_{12}, is defined as the velocity of the sprung mass (m_1) relative to the unsprung mass (m_2). The primary suspension is made up of a spring element, k_s, and a damper, c. Tire stiffness is represented by k_t. In order to implement the semi-active control, a magneto-rheological (MR) damper will be used in place of a passive damper. Many studies have shown the promise of MR technology for vehicle applications [14–17].

Following a review of skyhook, groundhook, and hybrid semi-active control policies, the test setup will be discussed. This includes a description of the quarter-car rig at the Advanced Vehicle Dynamics Laboratory (AVDL) at Virginia Tech. The MR damper used in this study will also be discussed along with its damping characteristics. Finally, the results of the study will be presented and conclusions will be drawn.

2. Semi-active control methods

For the sake of review, it is valuable to consider the equations governing skyhook and groundhook control. Recall for skyhook that the semi-active damping force is defined as

$$\begin{Bmatrix} v_1 v_{12} \geqslant 0 & F_{sa} = c_{sky} v_1 \\ v_1 v_{12} < 0 & F_{sa} = 0 \end{Bmatrix} \tag{1}$$

where,

v_1 = absolute velocity of the sprung mass
v_{12} = relative velocity across the suspension
F_{sa} = semi-active damping force
c_{sky} = skyhook damping coefficient (gain)

The equation governing groundhook control can be expressed as

$$\begin{Bmatrix} -v_2 v_{12} \geqslant 0 & F_{sa} = c_{gnd} v_2 \\ -v_2 v_{12} < 0 & F_{sa} = 0 \end{Bmatrix} \tag{2}$$

where,

v_2 = absolute velocity of the unsprung mass
c_{gnd} = groundhook damping coefficient (gain)

With hybrid control, the user has the ability to specify how closely the controller emulates skyhook or groundhook. In other words, hybrid control can divert the damping energy to the bodies in a manner that eliminates the compromise that is inherent in passive dampers. Combining the Eqs (1) and (2) we arrive at the semi-active hybrid control policy:

$$\begin{Bmatrix} v_1 v_{12} \geqslant 0 & \sigma_{sky} = v_1 \\ v_1 v_{12} < 0 & \sigma_{sky} = 0 \end{Bmatrix}$$
$$\{F_{sa} = G[\alpha \sigma_{sky} + (1-\alpha)\sigma_{gnd}]\} \tag{3}$$
$$\begin{Bmatrix} -v_2 v_{12} \geqslant 0 & \sigma_{gnd} = v_2 \\ -v_2 v_{12} < 0 & \sigma_{gnd} = 0 \end{Bmatrix}$$

where σ_{sky} and σ_{gnd} are the skyhook and groundhook components of the damping force. The variable α is the relative ratio between the skyhook and groundhook control, and G is a constant gain. Consider the case when α is 1; the control policy reduces to pure skyhook. When α is 0, the control is purely groundhook. Table 1 illustrates the ideal configuration of each of the control policies along with their respective governing semi-active control equations.

Table 1
Control policy identification

Control method	Governing equation	Idealized depiction
Skyhook	$\left\{ \begin{array}{ll} v_1 v_{12} \geqslant 0 & F_{sa} = c_{sky} v_1 \\ v_1 v_{12} < 0 & F_{sa} = 0 \end{array} \right\}$	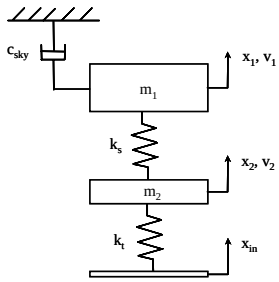
Groundhook	$\left\{ \begin{array}{ll} -v_2 v_{12} \geqslant 0 & F_{sa} = c_{gnd} v_2 \\ -v_2 v_{12} < 0 & F_{sa} = 0 \end{array} \right\}$	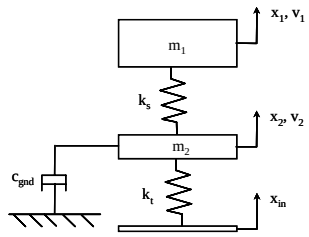
Hybrid	$\left\{ \begin{array}{ll} v_1 v_{12} \geqslant 0 & \sigma_{sky} = v_1 \\ v_1 v_{12} < 0 & \sigma_{sky} = 0 \end{array} \right\}$ $\{F_{sa} = G[\alpha \sigma_{sky} + (1-\alpha)\sigma_{gnd}]\}$ $\left\{ \begin{array}{ll} -v_2 v_{12} \geqslant 0 & \sigma_{gnd} = v_2 \\ -v_2 v_{12} < 0 & \sigma_{gnd} = 0 \end{array} \right\}$	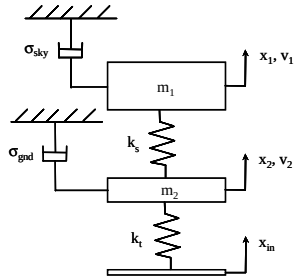

3. Test setup

The quarter-car rig at the AVDL was designed as a physical representation of a classic 2DOF system. In the physical implementation of the 2DOF model, each component of the quarter-car was chosen to closely resemble the characteristics of one quarter of a passenger vehicle. Figure 2 illustrates the primary components of the quarter-car rig. The unsprung mass is excited by a hydraulic actuator through eight elastomeric mounts. When mounted in parallel, the eight elastomeric mounts closely resemble the vertical stiffness of a tire.

The primary suspension stiffness was modeled by two air springs mounted in parallel. Air springs offer the ability to change the stiffness. However, the nonlinearity associated with airsprings had to be addressed. In order to maintain constant stiffness throughout the range of displacement across the suspension, the airsprings were connected to a 30-gallon tank which acted as a reservoir. This increased the total volume and helped to maintain near constant pressure throughout the closed-air system.

Table 2
System Parameters

Parameter	Value
Sprung Body Weight (m_1)	950 lbs
Unsprung Body Weight (m_2)	100 lbs
Suspension Stiffness (k_s)	200 lb/in
Tire Stiffness (k_t)	1085 lb/in

The sprung and unsprung masses were tuned to represent typical values for passenger vehicles. Table 2 summarizes the parameters used in testing. With these parameters, natural frequencies of the sprung and unsprung masses were 1.5 Hz and 10.5 Hz respectively. Figure 3 shows the undamped response of the quarter car rig, confirming these natural frequencies.

The inputs chosen for this portion of the study are derived from the undamped dynamics of the quarter-car rig. Two pure tone sine waves with frequencies at 1.5 Hz and 10.5 Hz were chosen to represent the steady-

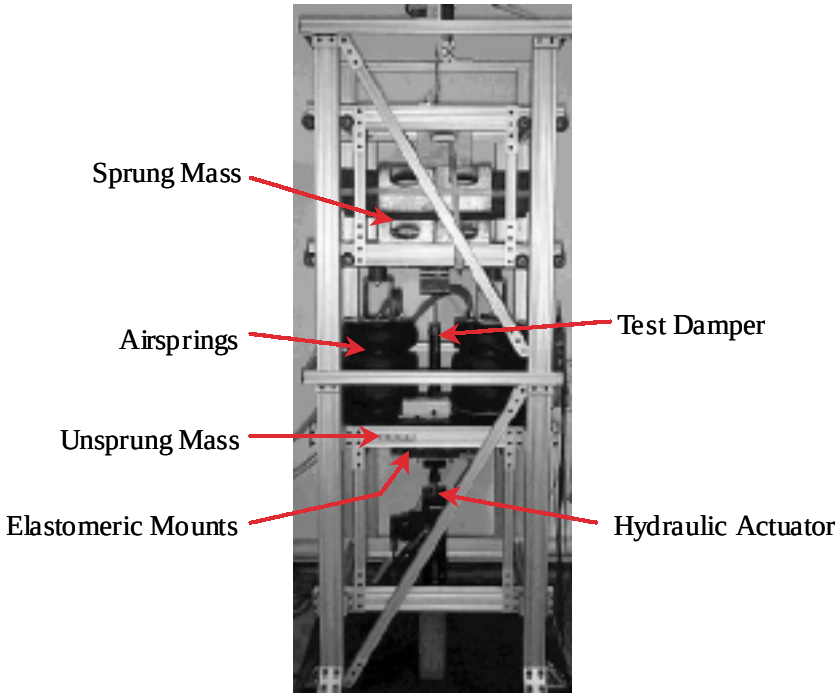

Fig. 2. Quarter-Car Rig and Primary Components.

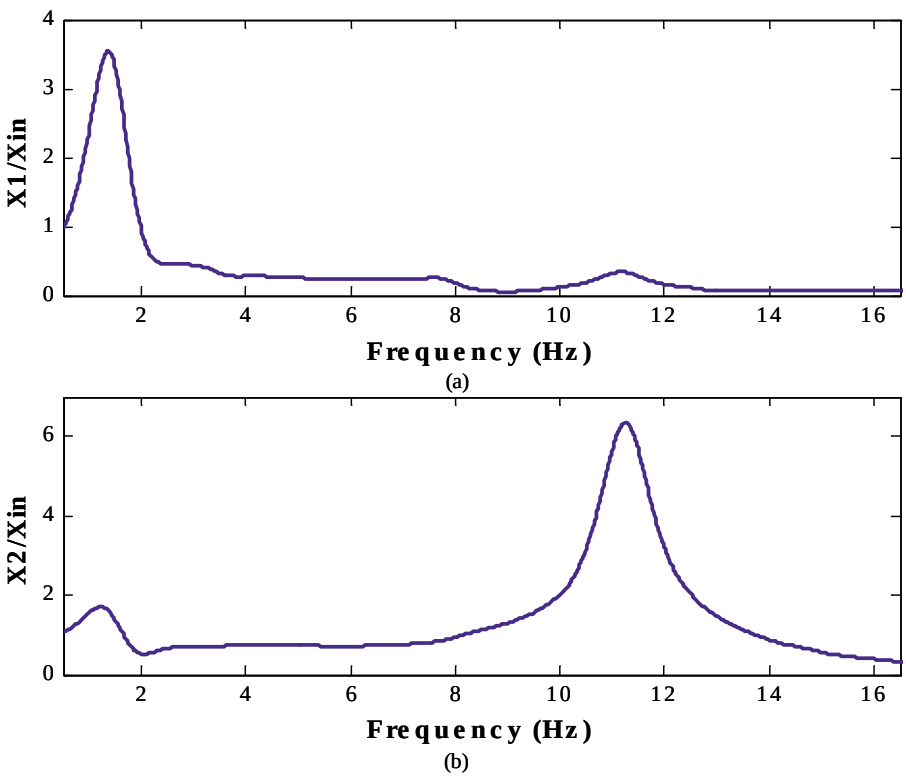

Fig. 3. Undamped Dynamics of the Quarter-Car Rig at 10 psi: (a) Sprung Mass Transmissibility; (b) Unsprung Mass Transmissibility.

state analysis. Because these frequencies are the natural frequencies of the sprung and unsprung masses, exciting the quarter-car rig at these frequencies resulted in the greatest response. Therefore, the ability or inability of the hybrid control policy to control the response to these inputs would be highlighted. In other words, this approach measures the performance at controlling the worst case scenario for both the sprung and unsprung masses.

The transient input chosen for this study was a step input. More accurately, it was a square wave with a frequency of 0.1 Hz. The low frequency of the square wave ensured that the responses of the sprung and unsprung masses to the input had died out before the next input sequence. With a total period of 10 seconds, there was a 5 second delay between the steps in the square wave. This delay ensured that all dynamics had died out before the next input. The amplitude of the step input was limited by the physical stroke of the MR damper. We wanted to maximize the input amplitude of the step function without hitting the end stops of the damper. A peak-to-peak amplitude of 0.9 inches was found to be sufficient.

The control signals necessary for semi-active control were measured using various transducers. Specifically, the velocities of the sprung and unsprung masses were measured using Linear Variable Differential Transformers (LVDTs). These transducers were also able to measure the displacement of both masses. Control was implemented using a dSPACE AutoBox. Through dSPACE, we were able to implement real time control and acquire experimental data.

The damper used in this study was a magneto-rheological (MR) damper built specifically for vehicle applications. A detailed discussion of the specifics of this damper can be found in the work by James Poynor [18]. The damper is shown in Fig. 4. All of the components have been incorporated internally, providing a compact design that is very similar in size and shape to existing passive vehicle dampers. The only external parts are the two electrical leads for the electromagnet, which are connected to the current source. Figure 5 shows the force velocity characteristics of this particular damper under several different operating currents.

4. Test results

A series of tests were performed on the quarter-car rig, in which the hybrid semi-active control policy was evaluated. The focus of this study is on the transient and steady-state dynamics of the hybrid semi-active suspension. Hybrid control was evaluated for its performance at controlling the sprung and unsprung masses according to the following two criteria:

- Peak-to-peak displacement
- Peak-to-peak acceleration

The peak-to-peak values can be expressed as:

$$PTP = \max(x(t)) - \min(x(t)) \tag{4}$$

where $x(t)$ is either the displacement or the acceleration of the sprung or unsprung masses. The displacement standards are valuable in considering the physical travel of each of the masses. This becomes particularly important for the unsprung mass. Large displacements at the wheel-hop natural frequency could lead to unsafe driving conditions. Criteria dealing with acceleration are catered to the sprung mass. Acceleration is the parameter by which ride comfort is commonly measured.

In evaluating the transient dynamics, it should be noted that the minimums and maximums are defined as the minimums and maximums of the response to a full step cycle. Specifically, the maximums and minimums of the response refer to the maximums and minimums of the overshoot as shown in Fig. 6. In this fashion, we are able to evaluate the dynamics of both a jounce step and a rebound step.

4.1. Steady-state analysis

The results for the steady-state analysis are presented for both displacement and acceleration. For comparison, the sprung mass peak-to-peak displacement is shown for an excitation of 1.5 Hz while the unsprung mass peak-to-peak displacement is shown for an excitation of 10.5 Hz. This approach is valid because exciting the sprung mass at the unsprung mass natural frequency, 10.5 Hz, would not reveal any profitable results because 10.5 Hz is well above the isolation frequency of the sprung mass. The same is true of the unsprung mass dynamics at 1.5 Hz.

Figure 7 shows the peak-to-peak displacement of the sprung and unsprung masses at their respective natural frequencies. The amplitudes are shown for two hybrid controller gains. As α increases from 0 to 1, the transition from groundhook control to skyhook control is evident. Clearly, hybrid control offers benefits to both the sprung and unsprung masses. The horizontal lines represent the peak-to-peak displacements of a passive

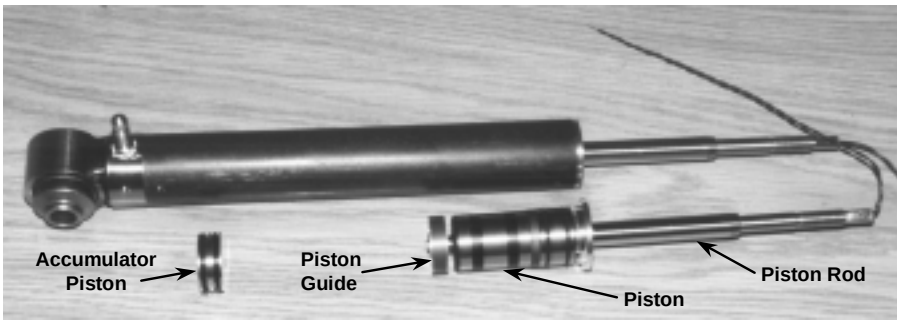

Fig. 4. MR damper and internal components.

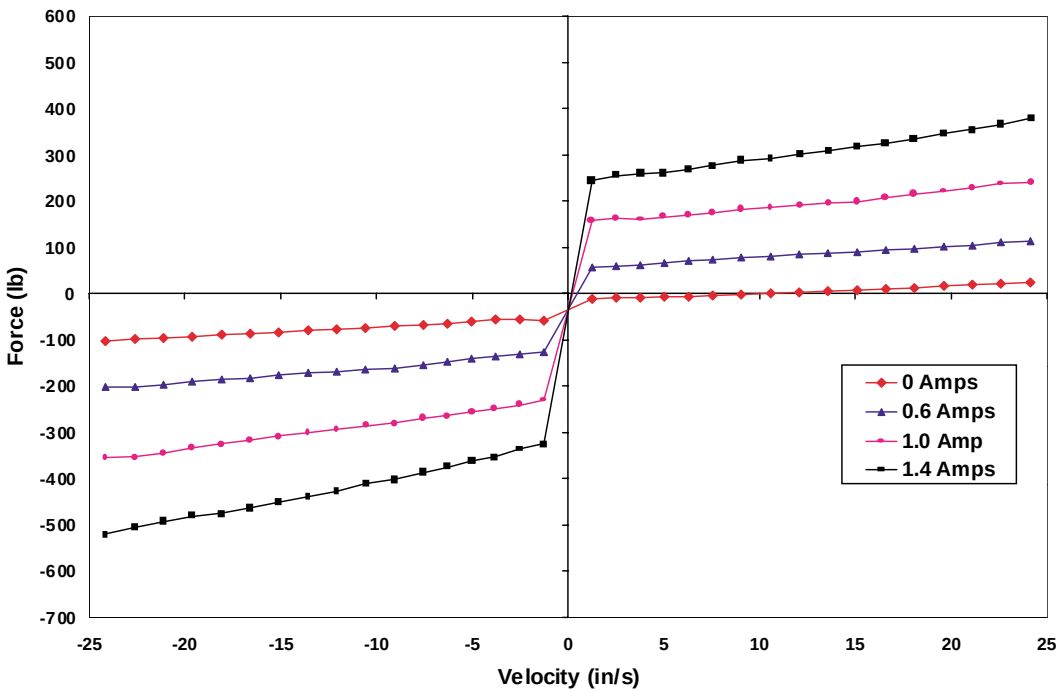

Fig. 5. MR Damper Damping Force Envelope.

system at the sprung and unsprung mass natural frequencies.

The peak-to-peak acceleration shown in Fig. 8 reveals similar results. As α is increased from 0 to 1, the sprung mass peak-to-peak acceleration decreases. The opposite is true for the unsprung mass when α decreases from 1 to 0. Here again, hybrid control reduces the response of both masses below that of passive.

In an attempt to view the effects of α and gain simultaneously, the amplitudes of the sprung and unsprung mass peak-to-peak displacements and peak-to-peak accelerations were compiled and plotted in a 3-D surface. The 3-D plots in Fig. 9 graphically illustrate the effect of α and gain for each of the criteria considered for both the sprung and unsprung masses. Clearly, when considering the sprung mass, the best choice would be $\alpha = 1$. Conversely, when the focus is the unsprung mass, an α of 0 offers the best performance. In both cases, the response decreases as the gain increases. It should be noted that for illustration, some of the axes orientations have been changed.

4.2. Transient analysis

Recall that the transient input used for this study was a step input. Just as in the steady-state analysis, hybrid control is evaluated according to the peak-to-

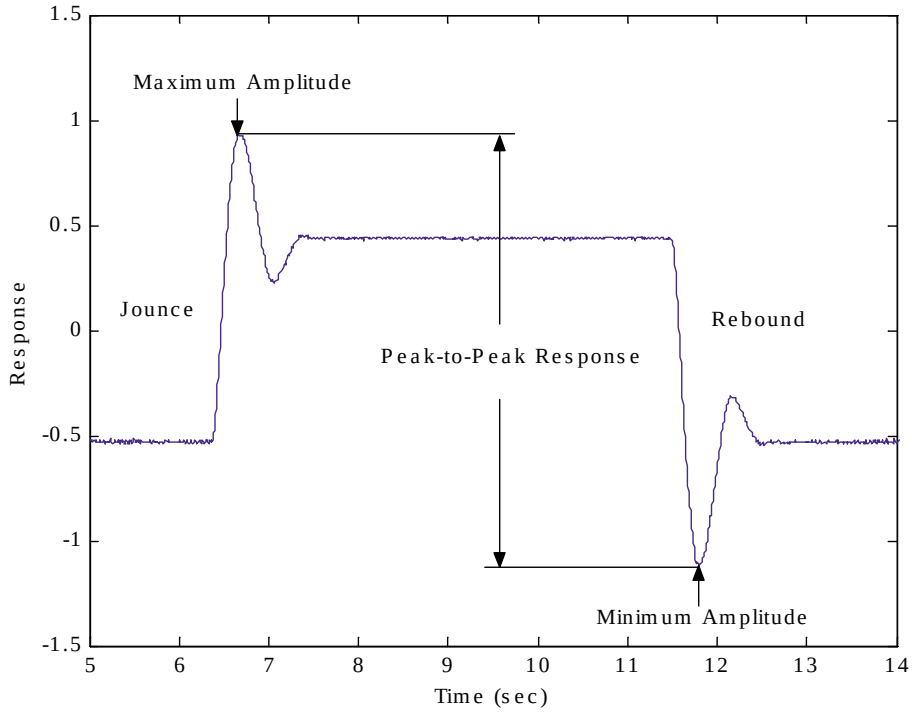

Fig. 6. Step Response.

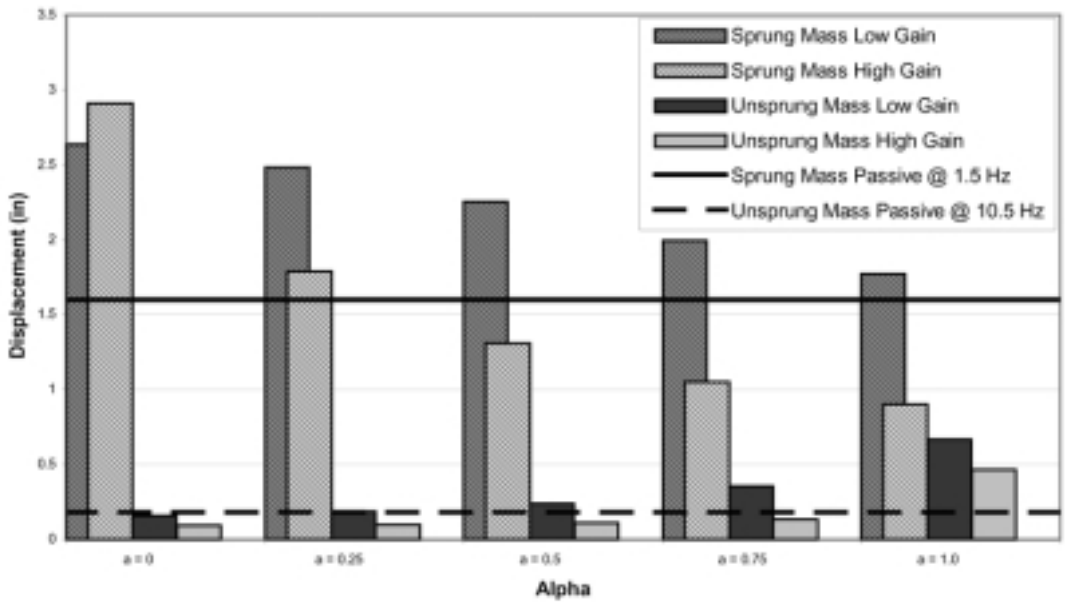

Fig. 7. Steady-State Peak-to-Peak Displacement.

peak displacements and peak-to-peak accelerations of both the sprung and unsprung bodies.

Figure 10 shows the peak-to-peak displacements of the sprung and unsprung masses to a step input. The transient response demonstrates similar results to those found in the steady-state analysis. The ideal configuration for the sprung mass is high α, high gain (i.e., skyhook control). Figure 10 also reveals that the bene-

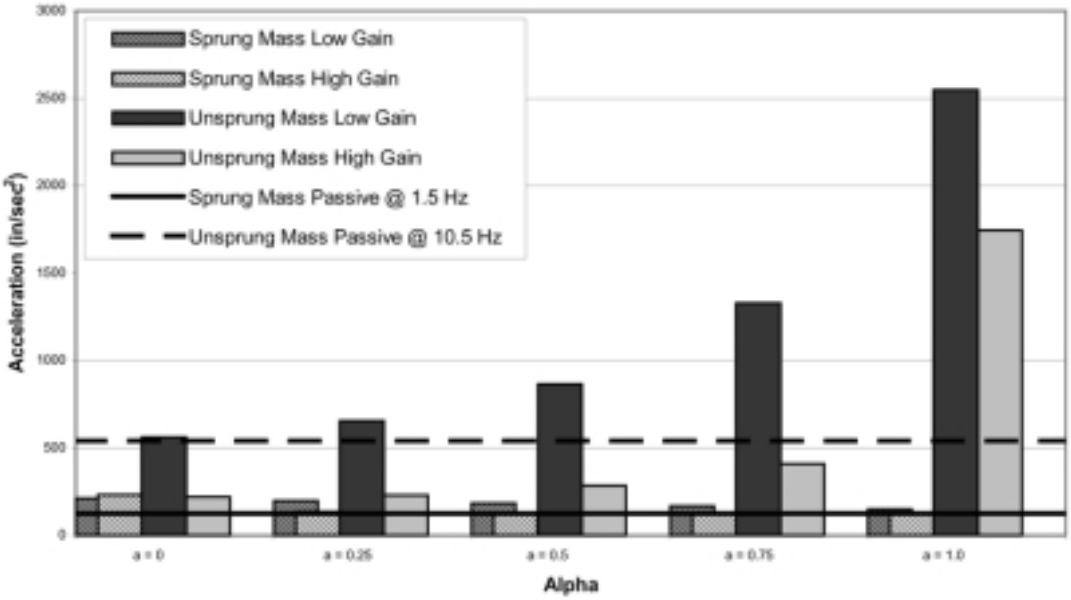

Fig. 8. Steady-State Peak-to-Peak Acceleration.

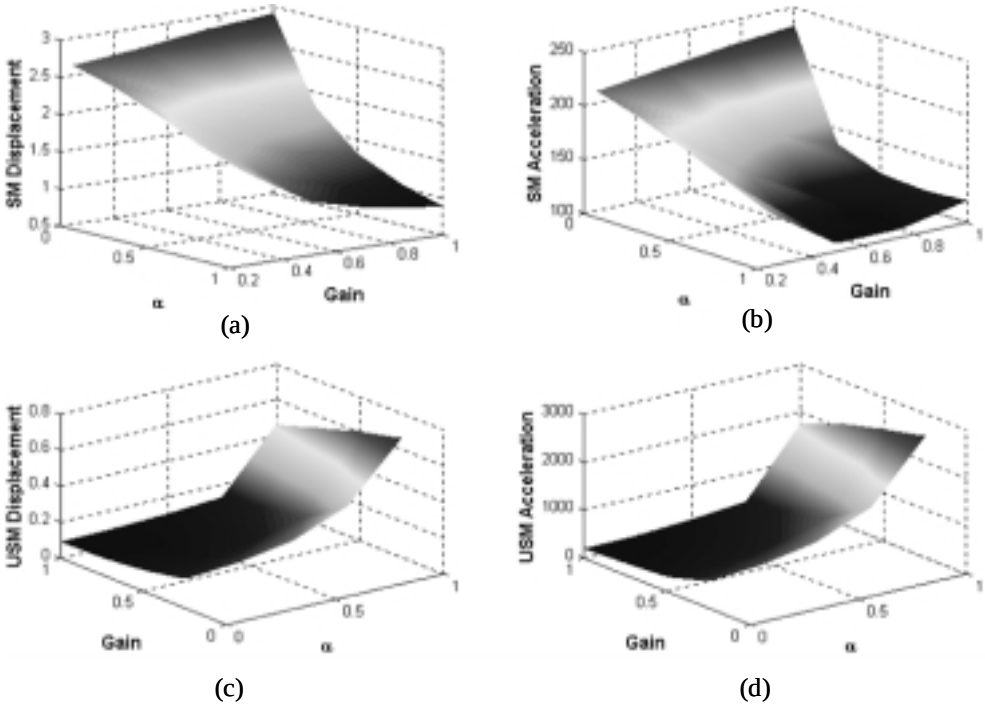

Fig. 9. Effects of α and Gain on Steady-State Response: (a) Sprung Mass Peak-to-Peak Displacement; (b) Sprung Mass Peak-to-Peak Acceleration; (c) Unsprung Mass Peak-to-Peak Displacement; (d) Unsprung Mass Peak-to-Peak Acceleration.

fits observed for the sprung mass far exceed those observed for the unsprung mass. Even at pure groundhook, $\alpha = 0$, the unsprung mass does not show much improvement over the range of alphas. Nonetheless, the peak-to-peak displacement of the unsprung mass is reduced below that of the passive system.

Peak-to-peak accelerations of both the bodies offer another means of evaluating the transient dynamics.

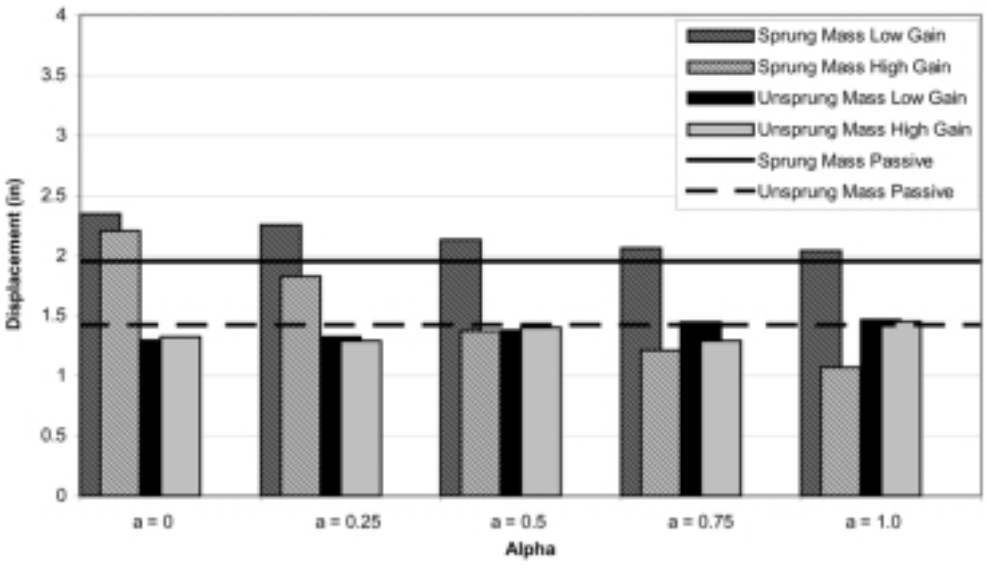

Fig. 10. Transient Peak-to-Peak Displacement.

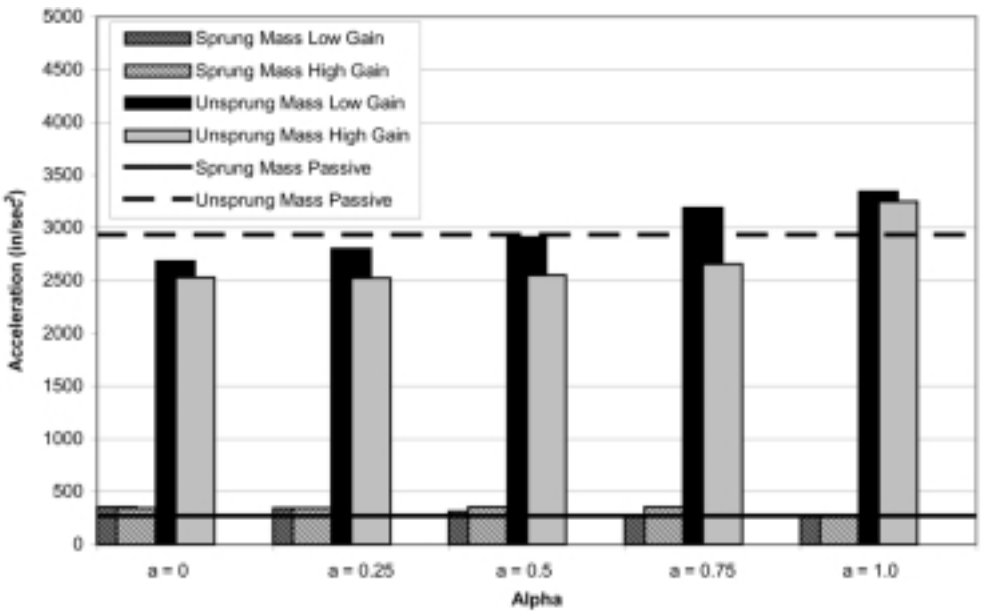

Fig. 11. Transient Peak-to-Peak Acceleration.

In Fig. 11, we observe that the unsprung mass now shows more improvement than the sprung mass as α is changed. The sprung mass acceleration remains relatively constant even as α approaches 1. Passive damping appears to offer better response than the hybrid control in several of the cases. The results in Figs 10 and 11 indicate that while hybrid control can reduce the peak-to-peak displacement of the sprung mass, there is no significant improvement in the sprung mass peak-to-peak acceleration.

Once again, the 3-D representation of the transient results helps to demonstrate the effects of α and gain simultaneously. Figure 12 summarizes the transient response results and confirms many of the observations made earlier. Moreover, the effect of gain on the peak-to-peak acceleration of the sprung mass is highlighted. Figure 12 reveals that the minimum peak-to-peak acceleration of the sprung mass occurs at low gain. This,

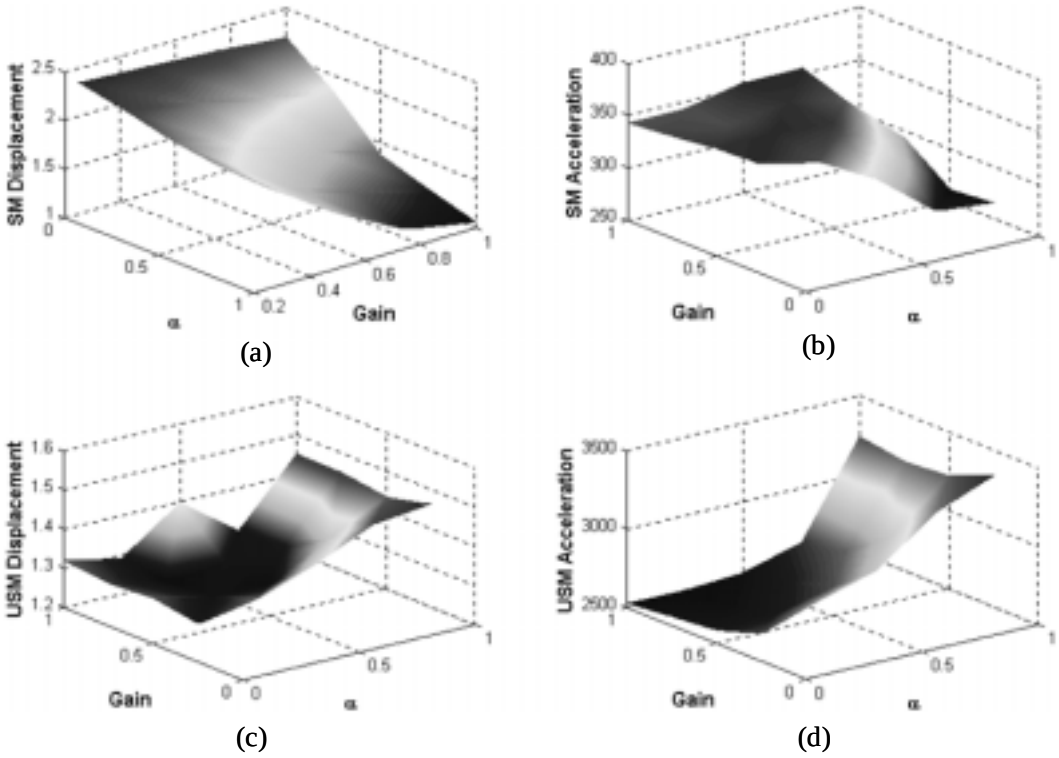

Fig. 12. Effects of α and Gain on Transient Response: (a) Sprung Mass Peak-to-Peak Displacement; (b) Sprung Mass Peak-to-Peak Acceleration; (c) Unsprung Mass Peak-to-Peak Displacement; (d) Unsprung Mass Peak-to-Peak Acceleration.

however, is not the case for the peak-to-peak displacement. The peak-to-peak displacement of the sprung mass decreases as gain is increased. Once again, some of the axes orientations have been changed to better illustrate the effects of changing each of the parameters.

5. Observations

This study further reveals the compromise present in semi-active suspensions. Whether the focus is on the sprung mass or the unsprung mass, hybrid control has been shown to offer benefits for both bodies. The compromise present in pure skyhook and pure groundhook can be reduced using hybrid control.

The steady-state results reveal that hybrid control can be used to reduce the peak-to-peak displacements and accelerations of both bodies. Even with an α of 0.5, both the sprung and unsprung mass responses are reduced below the response of passive. This implies that gains can be achieved using equal contributions from skyhook and groundhook (i.e., hybrid $\alpha = 0.5$).

The transient evaluation shows that hybrid control can be effective at reducing the peak-to-peak displacement of the sprung mass. However, the peak-to-peak acceleration of the sprung mass is not greatly affected by the hybrid control. In many cases, the peak-to-peak acceleration of the sprung mass under hybrid control is greater than that of passive. The unsprung mass acceleration, however, can be reduced using hybrid control. The peak-to-peak acceleration of the unsprung mass is reduced below that of passive under hybrid control.

6. Summary

The performance of hybrid control was studied experimentally under steady-state and transient inputs. Experimental results were obtained using a quarter-car rig and a magneto-rheological damper. The hybrid control policy was employed and evaluated under a steady-state, or pure tone, input and a transient, or step input. Peak-to-peak displacement and peak-to-peak acceleration were used to evaluate performance.

The results indicate that hybrid control can offer benefits to both the sprung mass and the unsprung mass. Both the steady-state and transient dynamics of the sprung and unsprung masses can be reduced below

those of passive using an α of 0.5. This corresponds to equal contributions from skyhook control and groundhook control.

References

[1] M.J. Crosby and D.C. Karnopp, *The Active Damper*, The Shock and Vibrations Bulletin **43**, Naval Research Laboratory, Washington, DC, 1973.

[2] D.C. Karnopp and M.J. Crosby, *System for Controlling the Transmission of Energy Between Spaced Members*, U.S. Patent 3,807,678.

[3] D. Hennecke, P. Baier, B. Jordan and E. Walek, *EDC III–The New Variable Damper System for BMW's Top Models – A Further Development of our Adaptive, Frequency-Dependent Damper Control*, SAE Technical Paper Series, No. 900662, Warrendale, PA, 1990.

[4] M. Ahmadian, Ride Evaluation of a Class 8 Truck with Semi-Active Suspensions, *Advanced Automotive Technologies, ASME Dynamic Systems and Control Division, DSC*, **52** (1993), 21–26.

[5] J. Lieh, W.J. Li, Adaptive Fuzzy Control of Vehicle Semi-Active Suspensions, *ASME Dynamic Systems and Control Division, DSC* Fairfield, NJ, **61** (1997), 293–297.

[6] H.C. Sohn, K.S. Hong and J.K. Hedrick, Semi-Active Control of the Machpherson Suspension System: Hardware-in-the-Loop Simulations, *Proceedings of the 2000 IEEE International Conference on Control Applications* Piscataway, NJ, **1** (2000), 982–987.

[7] A. Giua, C. Seatzu and G. Usai, Semi-Active Suspension Design with an Optimal Gain Switching Target, *Vehicle System Dynamics* **31**(4) (1999), 213–232.

[8] R. Gehm, Delphi Improves Cadillac's Ride, *Automotive Engineering International* **109**(10) (Oct, 2001), 32–33.

[9] D. Pund, F. Markus, A. Robinson and L. Webster, The New Cars, Charting the Changes for 2002, *Car & Driver* **47**(4) (Oct, 2001), 62.

[10] K.A. Wilson, Muscle from Modena, *AutoWeek* **51** (48) (Nov, 19th, 2001), 22.

[11] R. Hutton, Trio Appassionato: Ferrari FX, Lamborghini Murcielago, and Maserati Spyder, *Car & Driver* **47**(6) (Dec. 2001), 42.

[12] M. Ahmadian, *A Hybrid Semiactive Control for Secondary Suspension Applications*, Proceedings of the Sixth ASME Symposium on Advanced Automotive Technologies, 1997 International Congress and Exposition, November, 1997.

[13] D.E. Ivers and L.R. Miller, Semiactive Suspension Technology, *An Evolutionary View, ASME Advance Automotive Technologies, DE-40, Book No. H00719-1991*, 1991, pp. 327–346.

[14] H.S. Lee and S.B. Choi, Control and Response Characteristics of a Magneto-Rheological Fluid Damper for Passenger Vehicles, *Journal of Intelligent Material Systems & Structures* **11**(1) (January 2000), 80–87.

[15] F.L. Hiu and H.L. Wei, Semi-Active Control of Automotive Suspension Systems with Magnetorheological Dampers, *Proceedings of SPIE* **4327** (2001), 125–136.

[16] C.Y. Lai and W.H. Laio, Vibration Control of a Suspension System via a Magnetorheological Fluid Damper, *Proceedings of SPIE*, **4073** (2000), 240–251.

[17] F. Gordaninejad and S.P. Kelso, Fail-Safe Magneto-Rheological Fluid Dampers for Off-Highway, High-Payload Vehicles, *Journal of Intelligent Material Systems & Structures* **11**(5) (May, 2000), 395–406.

[18] J.C. Poynor, Innovative Designs for Magneto-Rheological Dampers, master's thesis, Blacksburg, VA, Virginia Tech, August, 2001, pp. 32–33.